Prediction of pharmaceutical blends flowability using a Schulze Ring Shear Cell tester

Maria M. Guedes[1,2], A. C. Diogo[1], Slavomira Doktorovova[2], Maria C. Paisana[2]
1- Instituto Superior Técnico, Lisbon, Portugal; 2- Hovione, Lisbon, Portugal

March 2022

Abstract

To properly design equipment that handles bulk solids, it is considerably important to be familiar with their fundamental properties, since the flow of these materials is subjected to a series of instabilities that can make processing them impossible. These fundamental properties can be obtained with shear testers. Therefore, this thesis has the objective of gaining knowledge on the tests performed with the Schulze ring shear tester RST-XS.s and the results obtained.

In the first part of this work, five pharmaceutical powders (flow function coefficient from 2.2 to 19.5 at pre-consolidation stress of 1kPa) are analyzed by the RST-XS.s using two shear cells (XS-Mr, XS-SV3) and two wall friction cells (XS-MW, XS-WL0). The purpose is to select which cells most accurately predict how these materials flow through different hoppers. The data obtained was treated mathematically according to Mehos[1] and validated by discharging the powders through hoppers with varying wall angles (15° to 45°). Results showed that the most adequate cells to characterize pharmaceutical powders are XS-Mr and XS-WL0.

In the second part, ten more powders with different pharmaceutical functions are analyzed to better understand the output from the RST-XS.s. Results showed that flowability must not be evaluated solely by the FFC ratio, and should consider other parameters such as particle shape and size distribution.

Finally, in the third part of this study, five pharmaceutical blends varying in active concentration (0 - 60 %(w/w)) were manufactured. After characterizing the blends, tablets were produced at different tableting conditions (varying feeder and turret speed) and a weight variation test was performed. Results showed small relative standard deviations, suggesting that these formulations are adequate for tableting with the Active Principal Ingredient used. Further investigations on the matter are suggested.
Keywords: Ring Shear Tester, Flowability, Shear Cell, Wall Friction Cell, Tableting.

1. Introduction

Many tests have been developed along the years to assess the flowability of bulk solids. [2] For example, the angle of repose test consists in pouring powder through a funnel placed above a plaque, forming a pile of loose powder, and measuring the slope of this pile. This plaque may have a lateral elevation to create a layer of powder and eliminate any possible interference that the plaque could have in the results. This angle can also be determined by measuring the angle of the pile of dust that remains in a container with a small opening on the bottom or by measuring a dynamic angle which is measured in a rotating cylinder. This last method is the least reliable one for materials with worse flowability. For instance, cohesive materials wouldn't flow continuously but in small avalanches.[3]

Carr's index and Hausner's ratio are indicators for the compressibility of a powder and are based on the influence of adhesive inter-particle interactions on the bulk density, ρ_{b0}, and relate this density with the density of the powder after compaction, ρ_T. A Carr's index of 0 or a Hausner's ratio of 1 indicate that the bulk solid under study is uncompressible, which corresponds to the best flowability possible. The bigger these values, the worse the flowability.

Other examples of empirical tests that are done are the measurement of the time of discharge of a bulk solid through a hopper with a small opening or the determination of the minimum size of the opening of the hopper through which there is flow of matter. For the first test, the smaller the discharge time, the better the flowability. For the second test, the minimum diameter of the opening of the hopper becomes an indicator for the flowability.[4][2]

Indeed, none of these techniques can be used to predict what will happen in practical applications, since theese tests do not simulate the necessary conditions. They may only be used to draw a comparison between samples, ordering them according to their flowability.

Today's equipment for shear testing is based on Jenike's shear tester and allows the measurement of powders' fundamental properties while the material

is under a consolidation stress that simulates the stresses existing in practical applications, unlike the other techniques described above.

Some other testers used throughout the history worth mentioning are the Warren Spring-Bradford cohesion tester, used to determine a value of cohesion of a powder that can be qualitatively compared to the values obtained for other powders [2][5]; the uniaxial compression test, in which the powder is pre-consolidated in a confined space and afterwards is compressed again, while being unconfined, until the point of incipient flow (the same as failure for a normal solid) [2][6]; the monoaxial shear tester, which is similar to the uniaxial compression tester, but after consolidating, a force is applied in the horizontal direction until the point of incipient flow [2][7]; the torsional shear tester, in which the sample is contained in a cylindrical cell and a vertical force is applied to the sample through a round lid with a roughened surface that rotates at a constant speed, allowing the measurement of the torque (M_M). [2][7] The equipment that will be used throughout this work, the ring shear tester, is a rotational tester, just like the torsional tester.

The most relevant parts of this equipment are a cell, where the powder sample is inserted with due care, a lid that generally has a rough surface to avoid slipping of the powder sample in the powder-lid interface and vertical loading rod that fits in the central axis of the lid, through which a vertical stress, F_N, is applied to the sample. This vertical stress consolidates the bulk solid sample while the basis of the powder cell rotates with a certain rotating speed, ω, causing the bulk displacement associated with shear. The lid is connected to the tie and push rods, which are connected to load sensors, measuring the forces F_1 and F_2 necessary to counteract the lid rotation. These forces F_1 and F_2 are directly proportional to the shear stress, τ. [2][8]

The geometry of the cell and lid varies according to the type of test to be performed.

1.0.1. Shear tests

The following information was processed from [9], [2].

In a Yield Locus test, the equipment applies a normal force F_N via the loading rod on the cross-beam of the lid, which is transmitted to the powder, consolidating it. The bottom of the cell then rotates clock-wise with a rotating speed of ω, generating a shear stress within the bulk of the powder. The bottom of the cell rotates until the shear stress value is constant, i.e. a steady state has been achieved. This is called the pre-consolidation state, where it is possible to obtain a pair of values of normal (σ) and shear (τ) stress, called the pre-shear point, where the normal stress is the one applied and the shear stress is the one at steady state. This first pre-consolidation stage is necessary, since bulk solids' history of consolidation influences the state of the powder, because the particles rearrange with every consolidation.

After achieving the steady state for the consolidation tension, all stresses are reduced to zero, meaning that the normal force applied is reduced to zero and the rotation of the bottom of the cell is reversed to the initial state.

From this point on, the second part of the test begins. In this part, a normal force lower than the consolidation tension is applied to the powder until the point of incipient flow. The equipment determines the incipient flow point, which, once again, corresponds to a pair of values of shear stress and normal tension, but this time, at incipient flow. This point is called a Yield Locus. The Yield Locus can be measured at various normal tensions (as long as they are lower than the consolidation tension) and a set of yield loci measured at different normal tensions forms a yield locus curve.

RST-XS.s allows the measurement of various Yield Loci per sample, which was a great achievement in collecting experimental data, as prior to this equipment large amounts of samples would be wasted, since only one Yield Locus point could be obtained per sample.

1.0.2. Wall friction tests

The main purpose of the wall friction test is to assess the tensions existing at the interface between the powder and the wall. This 'wall' would be the wall of the powder's container in a real situation, e.g. the internal wall of a storage silo.

In this test, the incipient flow of the powder is not assessed. Only steady-states are obtained. The functioning principle is the same as the Yield Locus test. A normal tension is applied with rotation of the cell until a steady state is reached. The difference is that in this test, this normal tension is reduced by increments, and for each normal tension applied, a steady state is attained, generating a set of points which will form the wall yield locus curve.

1.0.3. Motivation

It was mentioned before that the lack of knowledge of powder rheological and physical properties often leads to poor equipment design and equipment malfunction. There are two ways to approach these problems: either re-designing the equipment, which is very expensive, or optimizing the formulations used, so that they are adequate for the equipment used. This second option is the most common and cost-effective.[10]

Shear cell testers have been widely used in the pharmaceutical industry to characterize pharma-

ceutical powders and guide the development and optimization of formulations.

Throughout this work, a deeper understanding of *Schulze*'s ring shear cell tester *RST-XS.s* will be attained by analyzing different powders belonging to different pharmaceutical functional groups. Different pharmaceutical blends will be manufactured and tested with RSE-XS.s. In order to better understand the relationship between the rheological parameters obtained in shear testing and tablet weight variation, a set of tablets will be produced with these blends and weight variation will be assessed. A mathematical treatment model based on the literature will be be developed to predict whether pharmaceutical powders flow easily or not during their processing stages.

2. Implementation

The present work has been divided in three parts: in the first part, a selection of the most adequate cells to work with in further studies is made; next, a characterization of fifteen pharmaceutical powders is made, which, besides helping to better understand the way the equipment used works, will be used in the future as part of a database for pharmaceutical powders' rheology; and finally, a characterization of five blends is made, in order to understand how the rheological data obtained for the blends relates with the final tablet attributes.

2.1. Part I - Cell characterization

Five pharmaceutical powders (Flow Function Coefficient ranging from 2.2 to 19.5 at a pre-consolidation tension of 1 kPa) were selected: filler 1A (FMC Biopolymer), filler 2A (Meggle), filler 3 (Biogrund), binder 1A (Dow) and Active Principal Ingredient (API) 1 (Hovione).

A Schulze Ring Shear Cell Tester (*RST-XS.s*) with two shear cells (XS-Mr, XS-SV3) and two wall friction cells (XS-MW, XS-WL0) was used to assess these powders' fundamental properties. In this work, each powder was submitted to three shear tests at different pre-consolidation tensions (see Table 1).

Table 1: Vertical tensions applied during the three yield locus tests performed with each cell to each powder sample.

Test	σ_{pre} (Pa)	σ_{sh} (Pa)			
1	1000	300	500	800	300
2	2000	400	1000	1600	400
3	3000	600	1500	2400	600
4*	500	200	300	400	200

** When necessary. Not possible with cell XS-SV3.*

These tests were performed with an n=1, except for API 1, for which an n=3 was used, to assess the repeatability of the tests performed.

Wall yield locus tests were performed at a wall normal stress (σ_w) ranging from 50 Pa to 1 kPa with cell XS-WL0 and 250 Pa to 10 kPa with cell XS-WM.

The data obtained from the ring shear tester were treated mathematically according to Mehos[4] to calculate the value of the minimum outlet diameter that would allow mass flow in hypothetical hoppers, B_{min}. This calculation allowed the prediction of whether or not the powders would have mass flow in hoppers with an opening of 4 cm and varying vertical wall angle (45°, 30°, 25° and 15°). The mathematical results were validated by discharging the powders through hoppers with an opening diameter of 4 cm and different wall angles (45°, 30°, 25° and 15°).

The experimental data were also used to validate the Warren-Spring equation, by fitting the equation to the data and comparing the prediction of the values of σ_1 and σ_c to those obtained by the *RST-XS.s*.

2.2. Part II - Powder characterization

Ten additional pharmaceutical powders were analysed using cells XS-Mr and XS-WL0: Filler 1B (FMC Biopolymer); filler 1C (FMC Biopolymer); filler 2B (Meggle); filler 2C (KERRY); filler 4 (JRS PHARMA); binder 1B (Hovione); binder 2 (Hovione); API 2 (Fagron GmbH & Co.); lubricant 1 (PETER GREVEN); and disintegrant 1(DUPONT IE). Different grades of the same material are signalized with letters after the number that refers to the material itself.

Following the selection of the adequate cells to use in the first part, in this part, only cells XS-Mr and XS-WL0 were used. The yield locus tests performed in this part of the study were the same tests as the ones described in Table 1 (n=1). Vertical tensions for the wall yield locus tests performed were applied in the range between 50 Pa and 2 kPa. Each wall yield locus test was performed with five repetitions in one go, so although only one test was performed for each powder, the number of repetitions is equivalent to n=5.

The experimental data was, once again, mathematically treated according to Mehos [1].

2.3. Part III - Blend characterization

In the third part of this work, a set of five blends with increasing concentration of API (from 0 % to 60 %m/m) were analysed with Schulze's *RST-XS.s* following the same procedure used in Part II.

The experimental data from the *RST-XS.s* was treated mathematically according to Mehos [1] and a Principal Component Analysis (PCA) was ran in order to better understand the existing relation-

ships between the many parameters yielded on a yield locus or a wall yield locus test.

The five blends were prepared in a TURBULA® model T2F Shaker-Mixer at 32 rpm for 10 minutes. These blends were used to produce a number of tablets under different tableting conditions (varying turret and feeder speed) using a Riva Piccola classica with module, equiped with a forced feeder. A sample of 20 tablets from each condition was weighed and the relative standard deviation was calculated in order to find the relationship between weight oscillation and the results obtained with *RST-XS.s*.

3. Results

3.1. Part I - Cell characterization

The following figures show the flow functions obtained for the five powders tested with cell XS-Mr (1(a)) and with cell XS-SV3 (1(b)).

The results obtained with cells XS-Mr (Figure 1(a)) and XS-SV3 (Figure 1(b)) show that the shear cells do not yield the same results. In fact, cell XS-SV3 yields smaller shear stresses. The reason for this difference lies in the geometry of both cells and in the different surface characteristics. Due to the different surface of the lid of the XS-SV3 cell, the shear zone develops in a different way and becomes narrower within a shorter time. This results in a decrease of the shear stress compared to cell XS-Mr which has vanes at the lid.[11] In fact, Wang, et al. (2021)[12] state that cell geometry has a bigger impact on the results yielded for finer powders than for coarse powders. As a consequence, shear cell XS-SV3 yields results that correspond to a best-case scenario.

Since FFC is given by the ratio σ_1/σ_c, a flow function at lower unconfined yield strengths (σ_c) and major principal stresses (σ_1) has lower FFC, thus corresponding to a better flowability [13]. According to cell XS-SV3, filler 1A and binder 1A's flow functions are close to filler 2A's. Cell XS-Mr, on the other hand, yields higher flow functions for these two powders, being now in the middle of API 1 and filler 2A. This suggests once more that Cell XS-SV3 yields a best-case scenario.

It's worth mentioning that the order in flowability is maintained in both cells: API 1 having the worst flowability, followed by binder 1A and filler 1A, which are very similar, filler 2A and the one with the best flowability, filler 3. Thus, comparative studies can be performed with both cells as long as the same cell is used throughout the whole study [2][11].

Complementary data from the output of the equipment (bulk density, internal angle of friction) using the two cells also shows the same trend, decreasing from cell XS-Mr to cell XS-SV3.

Wall friction plots were obtained for each powder using the experimental data obtained from cells XS-WM and XS-SL0 combined. This plot is represented in Figure 2 with a linear XX axis and in Figure 3 with a logarithmic XX axis.

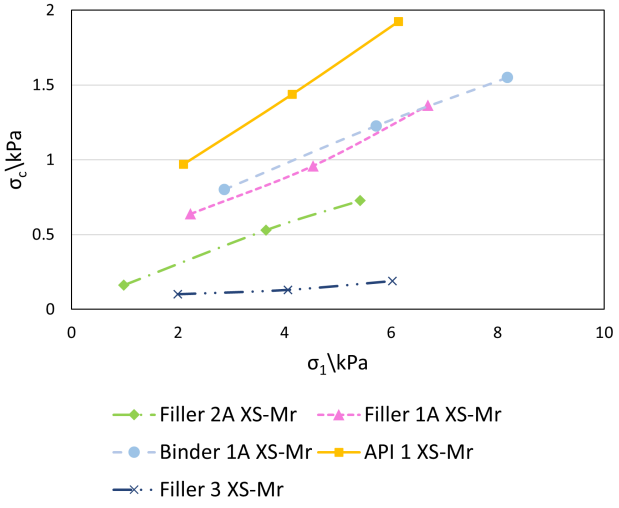

(a) Cell XS-Mr

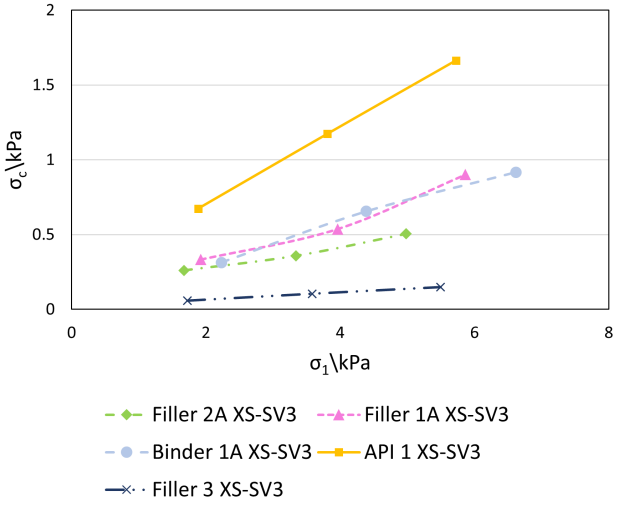

(b) Cell XS-SV3

Figure 1: Flow functions obtained with shear cells XS-Mr and XS-SV3.

Regarding the results obtained with the Wall Friction cells, it became clear that the decision of which cell to use must take into consideration not only the powder to be analyzed, but also the adequate normal tension range to be applied.

The shaded area shows the lower limit of XS-WM's σ_w range (194Pa to 23kPa), which does not comprise the initial part of the logarithmic plots, only covered by XS-WL0 cell (σ_w range: 0Pa to 13kPa). It's important to mention that some pharmaceutical operations performed at a smaller scale

than other industries have very small stresses associated [10], for example during the discharge of hoppers where values of σ_1 of less than 1kPa may be reached at times. This causes a need to extrapolate the plot for lower σ_W values when XS-WM wall friction cell is used.

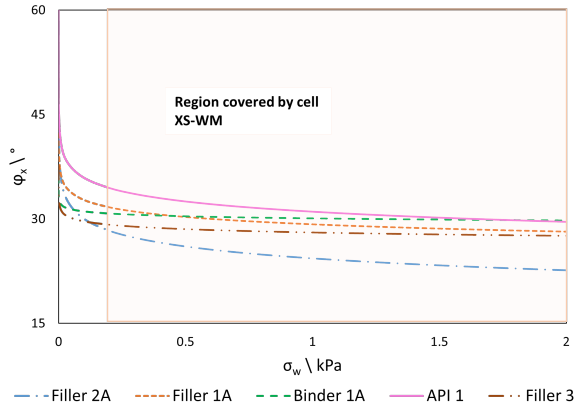

Figure 2: Curve $\varphi_X(\sigma_W)$ obtained for each powder with the data of cells XS-WM and XS-WL0 combined. Linear scale on the σ_W axis.

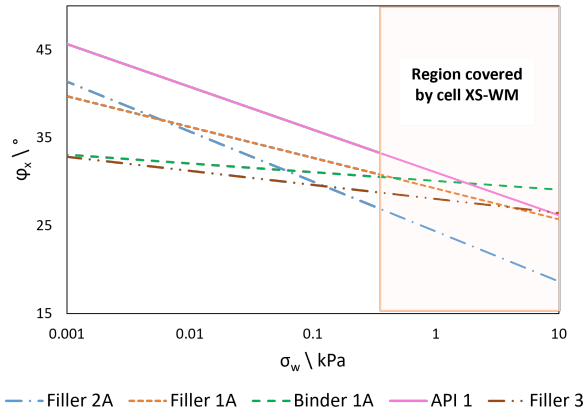

Figure 3: Curve $\varphi_X(\sigma_W)$ obtained for each powder with the data of cells XS-WM and XS-WL0 combined. Logarithmic scale on the σ_W axis.

In fact, generally the normal stress existing at the wall is considerably smaller than the major stress in the bulk [2]. Further calculations showed that the range of σ_W at the lab-scale and industrial scale bins considered will not be higher than 1.513kPa, which is still in the range of tensions that cell XS-WL0 can apply, but it will be lower than 120Pa, which is no longer in the range of cell XS-WM.

The mathematical treatment was applied to the five powders analysed and filler 1A, binder 1A and API 1 were predicted to have mass flow using the experimental data obtained with cell XS-Mr and with cell XS-SV3. These predictions were accurate for the three powders and corresponded to reality when flowing these powders through the lab-scale bins.

At first, the values obtained with the data from both cell XS-Mr and cell XS-SV3 predicted that there would be arching in every hopper. After validation, these predictions did not agree with experimental findings, so another point with a lower pre-consolidation tension was measured using cell XS-Mr (test 4 on Table 1). After obtaining the lower point it became obvious that the measurement made for test 1 shall be considered as an outlier, as shown in Figure 4. Since cell XS-SV3 has a lower limit of appliable normal tensions of 275 Pa, it wasn't possible to perform test 4 with this cell.

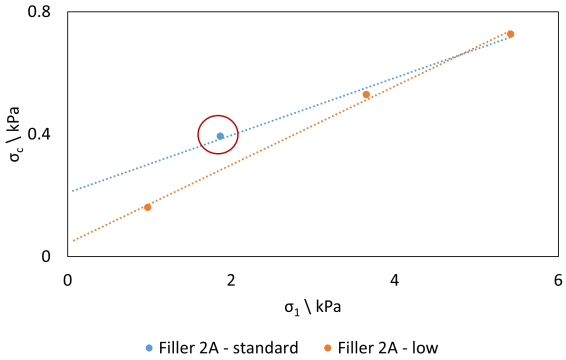

Figure 4: Flow functions for filler 2A obtained without test 4 (Standard) or with test 4 (Low).

Based on the new point from cell XS-Mr, the model predicted funnel flow in all hoppers. After validation, it was verified that there was indeed funnel flow in the hoppers with vertical wall angles of 45° and 30°, mixed flow in the hopper of 25° and mass flow in the one of 15°. The rathole diameter, D_F, was calculated, having the value of 4.1 cm. This diameter is very close to the actual outlet diameter of the validation funnels, which means that the prediction is very close to experimental results.

For Filler 3, the prediction using data yielded with cell XS-Mr was of funnel flow in all hoppers, while the prediction using data from cell XS-SV3 was of mass flow. Once again it is evidenced that cell XS-SV3 presents a best-case scenario. After validation, it was verified that there was indeed funnel flow in the hopper with vertical wall angle of 45°, mixed flow in the hoppers of 25° and 30°, and mass flow in the one of 15°.

It is worth noticing that with any shear tester, yield loci can be determined more accurately for more cohesive powders than for free-flowing ones, as would be the case of filler 3 and filler 2A, since the shear stresses are higher and thus the yield locus lies at higher shear stresses, so that small differences occurring from test to test

have less (relative) influence on the size of the unconfined yield strength stress circle and, thus, on unconfined yield strength. Furthermore, for free- or good-flowing materials often more extrapolation is required to determine the unconfined yield strength which increases the influence of fluctuation of the individual shear points further. The result is the tendency the less cohesive a material is, the more the unconfined yield strength fluctuates from test to test.[11]

The fit of the equation of Warren-Spring to the experimental data was assessed and successful and the prediction of the values of σ_1 and σ_c had a very reasonable accuracy and precision (deviation between the results from both reasonings in the range of 10^{-6} to 10^{-2}). This equation is essential in the analysis and prediction of important parameters for the design of silos (σ_1, σ_c), which allow the good design of silos, avoiding the risk of negatively impacting the final product due to arching or funnel flow problems.

The deviation between the results obtained in this mathematical treatment and the results included in the output of the equipment *RST-XS.s* was also calculated and it was verified that the values of τ_c and σ_c are the ones that most deviate from those obtained by the equipment (deviations in the order of 10^{-2} to $10^{-}1$), while the σ_1 values calculated via both reasonings used only had deviations in the order of $10^{-5} - 10^{-3}$ (reasoning 1) and of $10^{-4} - 10^{-2}$ (reasoning 2).

The deviations in the values of τ_c and σ_c can be explained due to the fact that the Warren-Spring curve is being fitted to three points only and that these three points are not in a low shear zone. This way, there is a big extrapolation of the data in the lower normal tensions zone, inducing a higher error in these calculations. These values of σ_1 however, take into consideration two extra points – the center of the circle and the pre-shear point. Having the pre-shear point enter the calculations is very important, since between each yield locus test, the sample is sheared back to the steady state, in order to ensure test reproductibility, thus the pre-shear point is the reference point for the yield locus tests made.

It was possible to notice a logarithmic correlation between the values of the curvature coefficient, n, and flowability. In fact, the lower the FFC, the higher the value of n which is coherent with the literature [14]. It is worth mentioning that the more cohesive a powder is, the more pronounced is the curvature of the Warren-Spring curve and thus, the more difficult is the fitting of the equation to the three non-low shear data points. This way, the repetition of these tests in future works is suggested, with lower consolidating stresses and a higher number of data points. However, it must be noticed that in practice, the way the tests are designed using the *RST-XS.s* does not allow the user to perform a great number of tests and obtain many points, since the same sample is used throughout the whole set of tests and slight physical degradation may occur in each test due to the compression forces applied. In the case where a normal tester is used, where one point is obtained per sample, the problem lies with the quantity of material used and a small quantity of tests will be performed to not waste too much of it. Therefore, there is an equilibrium to be taken into account between the accuracy of the Warren-Spring prediction of the cohesion and tensile strength parameters and the amount of powder used or its physical degradation.

Nevertheless, the equation presents a good fit to the experimental data and may be used in the future to predict the Mohr circles' placement and the values that may be calculated from them.

3.2. **Part II - Powder characterization**

A flow function at lower unconfined yield strengths and major principal stresses has lower FFC, thus corresponding to a better flowability [13]. This way, looking at Figure 5, it is possible to see that binder 1B presents the worst flowability, while filler 3 is the one that flows easier. In fact, API 2 is the one that presents the worst flowability of all 15 powders tested. However, it was removed from Figure 5 due to its high values of σ_1 and σ_c, improving the resolution of the plot for the other flow functions.

Effect of particle shape

Binder 1A, disintegrant 1 and filler 1A have elongated particles, reaching considerably higher σ_1 values for each pre-consolidation tension than the other powders.The elongated particles tend to reorientate when subjected to normal tensions, affecting force transmission and frictional behaviour. These particles tend to orient themselves in flow-direction, perpendicular to the major principal stress' direction, which allows for a higher compaction and, consequently, higher values of σ_1.[15] This effect is very evident in filler 1A, which has the most elongated particles.

Azéma et al. [16] found that φ_E varies nearly linearly with the elongation parameter, which is related to the aspect ratio, since there is an increase in friction forces and contact orientations with the increase of this parameter. Once again, this effect is most visible in filler 1A.

These elongated particles show higher φ_X values, with filler 1A having the highest values.

API 2 is the powder that exhibits the highest an-

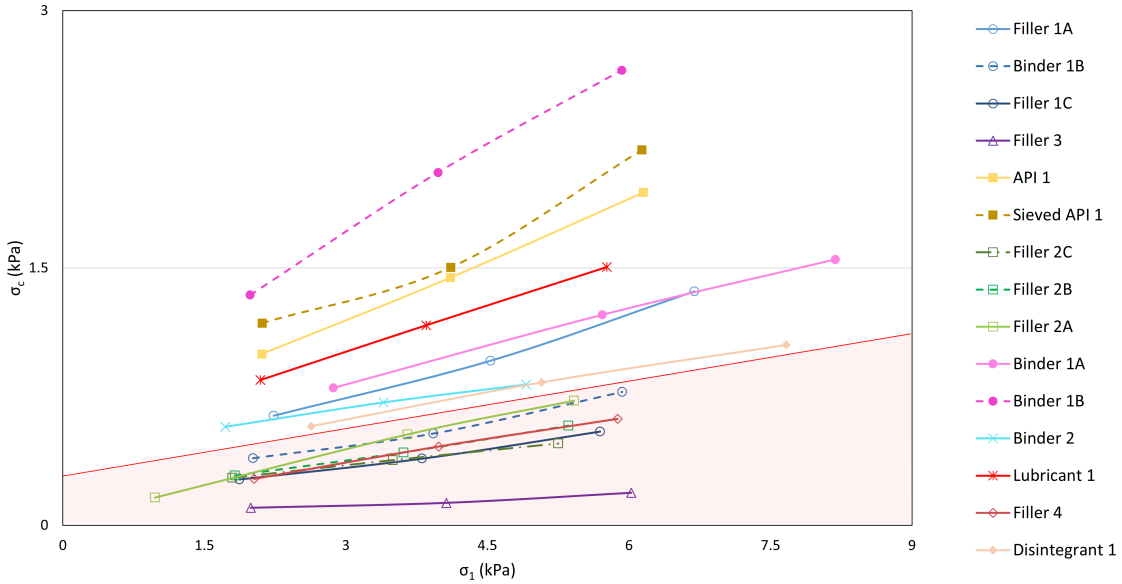

Figure 5: Flow functions obtained with cell XS-Mr for all powders tested except for API 2. The shaded region of the plot separates the fillers from the other powders tested.

gles of internal friction of all the fifteen powders tested, being the powder with stronger friction in the bulk. This API is made of a fraction of elongated angular particles and, as discussed before, the higher the elongation factor, the higher the φ_E, as well as the higher the level of angularity of a particle, the higher the φ_E [17][2]. Therefore, the shape of API 2's particles could explain the high values of φ_E that this powder demonstrates.

Lubricant 1 has plate-like particles that have both a polar and a lipophilic part. These particles delaminate and the lipophilic part is oriented so that waxy hydrophobic layers are formed. The low-friction characteristic of this powder is due to the weak links between the layers formed, allowing them to slide relatively to each other. This also allows the particles to coat adjacent particles when making blends, which lowers the bulk and wall friction of the blend as a whole. [18][19]

Effect of Particle size

Results show that the internal friction angles for filler 2B, filler 4 and filler 1C are very similar (maximum deviation from average of 1.6%), which suggests that particle size does not have a strong influence in the effective internal friction angle or at least not in this size range. This conclusion is in agreement with what was investigated by Liu, et al. (2015) [20].

It was noticed that with the filler 1 powders there is a trend where larger particles lead to lower friction angles. However, the inverse trend is observed for the filler 2 powders.

Both binder 1B and API 2 stand out for having higher unconfined yield strengths, followed by API 1 and lubricant 1. API 2 has the smallest particle size of all the powders studied and its particles are cristalline and angular, while binder 1B is also composed of small-sized particles and its particles have a shriveled surface. Having these irregular surface shapes, adjacent particles can establish a high number of interparticle contacts, which results in an increase in unconfined yield strength according to Johanson et al. [21], for small stresses.

Effect of fines content

A trend is seen among the filler 2 powders, where an increase in finer particles content leads to an increase in φ_E. This trend is in agreement with the literature, which states that for powders with particle sizes of smaller order (Pharmaceutical powders, for example), generally, the increase in fines content is unfavorable to flowability properties [2], while for powders of larger particle sizes (sand, for example), an increase in fines content leads to a decrease in the internal friction angle. [22]

Mathematical treatment

The results for B_{min} obtained for each powder studied are presented in Table 2.

3.3. Part III - Blend characterization

Characterization

From blends 1 through 4 there is a gradual increase in σ_c and in σ_1, which was to be expected,

Table 2: B_{min} calculated for a hopper with a vertical wall angle of 30°.

Powder	B_{min} (cm)
Binder 1A	23.2
Binder 2	26.7
Binder 2A	105.6
Lubricant 1	46.2
Disintegrant 1	15.7
API 1	32.9
Sieved API 1	39.8
API 2	258.9
Filler 1A	27.9
Filler 1B	14.7
Filler 1C	9.9
Filler 3	3.3
Filler 4	3.4
Filler 2A	funnel flow*
Filler 2B	6.5
Filler 2C	7.2

*Critical rathole diameter of 4.1 cm

since the quantity of API used (API 1) with a small particle size and angular particles is increased and the materials with best flowability were reduced. Even though Blend 5 has the same amount of API 1 as Blend 3, its flow function is very similar to that of Blend 4, which means that the replacement of filler 3 for filler 1B and glidant 1 had a considerably negative impact on flowability.

It is possible to observe an increase in bulk density from blends 1 to 4, which was to be expected, since API 1 (ρ_{b0}=0.48 g/cm^3)is one of the powders tested with higher bulk density and higher compressibility. Blend 5 however shows a great reduction in bulk density compared to Blend 3, which comes from the substitution of filler 3 (ρ_{b0}=0.41 g/cm^3) by filler 1B (ρ_{b0}=0.34 g/cm^3) and glidant 1 (ρ_{b0}=0.048 g/cm^3).

The wall friction angle was mostly unaffected by the addition of API or the substitution of filler 3.

The B_{min} values were calculated for all the blends and are presented in Table 3.

Table 3: B_{min} calculated for the blends for a hopper with a vertical wall angle of 30°.

Blend	1	2	3	4	5
B_{min} (cm)	6.0	7.4	7.7	8.4	8.8

Tableting and weight variation

Figures 6 and 7 represent the standard deviations associated with each batch produced. Both figures represent the same set of data, but in different displays, to ease interpretation. In Figure 6, the RSD is represented for each blend, varying in terms of turret/feeder speed. In Figure 7, the RSD is represented for each condition, varying with the blends.

No patterns were detected in Figure 6, suggesting that turret and feeder speed may have no influence on tablet weight variation. However, in Figure 7, there is a consistent increase in RSD from blends 2 to 4, suggesting that the increase in the content of the poorly flowing API and, therefore, the increase in bulk density and cohesion, does influence the weight variation, increasing it. These findings are coherent with the literature. [23]

In fact the relative standard deviations obtained for the tablets weighed are very low, considering that the European Pharmacopoeia states that when performing a mass uniformity test, "the tablets comply with the requirements if not more than 1 individual mass is outside the limits of 85–115% of the average mass. The tablets fail to comply with the test if more than 1 individual mass is outside these limits, or if 1 individual mass is outside the limits of 75–125% of the average mass." [24] In this case, the highest absolute deviation of an individual tablet's weigh to the average mass is of 2.6%.

The low deviations suggest once again that the blend used might be a good blend to produce tablets with API 1. However, we must not discard the possibility of having had a better-than-average batch of API 1. Therefore further studies should be made on these formulations and API.

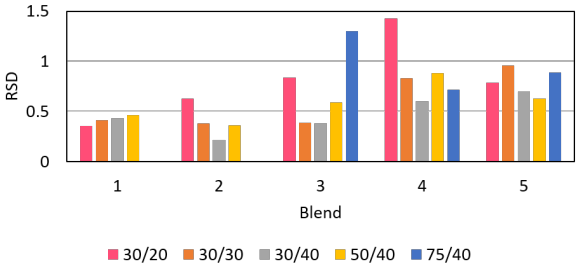

Figure 6: Relative standard deviation to the average tablet weight obtained for each tableting condition and each blend, varying the turret and feeder speed for each blend.

4. Conclusions

Results from Part I showed that XS-Mr generates higher cohesion values for powders than XS-SV3, and the latter represents, in general, a best-case scenario in terms of minimum orifice for powders to flow. XS-WL0 wall friction shows to be more adequate at smaller stresses, and therefore more representative of smaller scale processes. Also, this cell covers a wide range of compression tensions and can be used also for large scale processes, being

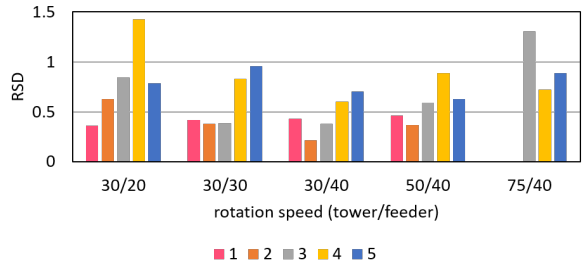

Figure 7: Relative standard deviation to the average tablet weight obtained for each tableting condition and each blend, varying the blend for each condition.

more versatile than XS-WM. Therefore, the most adequate cells to analyse pharmaceutical powders from the four cells studied are cell XS-Mr and cell XS-WL0. It is important to mention that for comparative purposes of flowability characterization, the same cells must be used throughout the whole study, since the geometry of the cells impacts the flow profile of the powder inside the cell. This difference particularly crucial when comparing cells XS-Mr and XS-SV3, since their volumes are considerably different, as well as the geometries in the base and lid. Besides this, further studies should be made with cell XS-Lr0 as well, to understand the advantages of this cell over the two shear cells used.

The fit of the equation of Warren-Spring to the experimental data was assessed and successful and the prediction of the values of σ_1 and σ_c had a very reasonable accuracy. An accurate prediction of the values of σ_c and σ_1 was to be expected, since some research has already been done on this topic and had good results. However, in this work, it was seen that the equation has a good fit to the data of not only cohesive powders, but also free-flowing ones. This equation can also be used to predict the values of cohesion (τ_c) and tensile strength (T). For these predictions to be accurate, more than three compression points must be used to trace the yield locus curve and approximate the curvature coefficient of the Warren-Spring equation. However, it must be noticed that in practice, the way the tests are designed using the *RST-XS.s* does not allow the user to perform a great number of tests and obtain many points. Therefore, there is an equilibrium between the accuracy of the Warren-Spring prediction of the cohesion and tensile strength parameters and the amount of powder used or its physical degradation.

In the second part of this work, it is proved that flowability should not be evaluated only by the FFC ratio, but should consider also other shear properties, wall shear parameters and particle shape and size. It is also observed that the equipment yields results that are coherent with the characteristics of the powders tested and meet the expectations. In further studies, the results obtained by mathematically treating the data in this section should be validated by flowing the powders through hoppers, as it was done in part I. However, this would imply having a large quantity of all powders tested.

The adapted mathematical model was successfuly adapted and can be used to compare the flowability of powders in silos by comparison of Bmin, the mininum outlet diameter of a hopper that allows mass flow. This parameter is more adequate than FFC to compare the flowability of powders in the same hypothetical bin, since it takes into account many factors that FFC does not, such as the internal friction angle or the wall friction. Nonetheless, care should be taken when analysing the output of the model, since it can also mean that there will be arching or funnel flow. It is also necessary to give an adequate input to the model, with at least three data points. This chapter made it possible to build a uniform database of flowability data for pharmaceutical powders. This mathematical model together with the Warren-Spring equation are useful tools that were proved to be very useful in the design of silos and hoppers.

Finally, in Part III, we see that using blends designed for having excellent flowability characteristics, such as the ones formulated for this work, has a great impact on the flowability of the API containing blends, decreasing the B_{min} value for a hypothetical hopper with a vertical wall angle of 30° from 32.91 cm (B_{min} estimated for API 1) to 8.4 cm (B_{min} estimated for Blend 4, which contains the highest quantity of API). This part of the work suggests that the formulations used might be indicated for direct compression with this API, since the blends showed great results in terms of rheological tests (Blend 4, with the highest quantity of API had results similar to those of Filler 2B) and and weight variability tests (RSD values below 2.6%) . However, it must be noticed that there might be a chance that the batch of API 1 used was better-than-average in terms of flowability. The quantification of these characteristics is deserving of a more thorough study, hence the author leaves as a suggestion for further studies the investigation on API 1 and the use of the blends mentioned for formulations with this API.

Acknowledgements

A big thank you to Instituto Superior Técnico, to Hovione and to my mentors, Professor António Correia Diogo, Slavomira Doctorovová and Maria Paisana, for your guidance, for always trying to make the best out of this project and for making me be in my best intellectual shape.

Finally, I would like to thank Dr. Dietmar Schulze and Dr. Greg Mehos for their help and

availability. Thank you for kindly answering our questions.

References

[1] Greg Mehos. Hopper Design Workbook, 2021. [Accessed June 2021].

[2] Dietmar Schulze, editor. *Powders and Bulk Solids: Behavior, Characterization, Storage and Flow*. Springer, Berlin, 1st edition, 2010.

[3] Hamzah M. Beakawi Al-Hashemi and Omar S. Baghabra Al-Amoudi. A review on the angle of repose of granular materials. *Powder Technology*, 330:397–417, 2018.

[4] CouncilOfEurope. *European Pharmacopoeia supplement 5.3*. European Directorate for the Quality of Medicine, 5th edition, 2005.

[5] J. Schwedes and D. Schulze. Measurement of flow properties of bulk solids. *Powder Technology*, 61(1):59–68, 1990.

[6] Don McGlinchey. *Characterisation of Bulk Solids*. Blackwell Publushing, Oxford, 1st edition, 2005.

[7] Jörg Schwedes. Review on testers for measuring flow properties of bulk solids. *Granular Matter*, 5:1–43, 05 2003.

[8] Dietmar Schulze. Ring Shear Tester RST-XS.s - Operating instructions v1.2 , 2019. [Accessed October 2021].

[9] Greg Mehos, editor. *STORAGE AND HANDLING OF BULK SOLIDS*. www.mehos.net, Westford, MA, 1 edition.

[10] Søren V Søgaard, Troels Pedersen, Morten Allesø, Jørgen Garnæs, and J Rantanen. Application of Ring Shear Testing to Optimize Pharmaceutical Formulation and Process Development of Solid Dosage Forms. *Annual Transaction of the Nordic Rheology Society*, 21:91–97, 2013.

[11] Dietmar Schulze. Private information.

[12] Chenguang Wang, Sichen Song, Chamara A. Gunawardana, David J. Sun, and Changquan Calvin Sun. Effects of shear cell size on flowability of powders measured using a ring shear tester. *Powder Technology*, 396:555–564, 2022.

[13] Jauhari Ashish, Gharde Swaroop, and Kandasubramanian Balasubramanian. Effect of ammonium perchlorate particle size on flow, ballistic, and mechanical properties of composite propellant. *Nanomaterials in Rocket Propulsion Systems*, pages 299–362, 1 2019.

[14] M. D. Ashton, D. C.-H. Cheng, Robert J. Farley, and F. H. H. Valentin. Some investigations into the strength and flow properties of powders. *Rheologica Acta*, 4:206–218, 1965.

[15] H. Ouadfel and L. Rothenburg. 'Stress–force–fabric' relationship for assemblies of ellipsoids. *Mechanics of Materials*, 33(4):201–221, apr 2001.

[16] Emilien Azéma and Farhang Radjaï. Stress-strain behavior and geometrical properties of packings of elongated particles. *Phys. Rev. E*, 81:051304, May 2010. [Accessed October 2021].

[17] Kunio Shinohara, Mikihiro Oida, and Boris Golman. Effect of particle shape on angle of internal friction by triaxial compression test. *Powder Technology*, 107:131–136, 01 2000.

[18] Praveen Hiremath, Kalyan Nuguru, and Vivek Agrahari. Material attributes and their impact on wet granulation process performance. *Handbook of Pharmaceutical Wet Granulation: Theory and Practice in a Quality by Design Paradigm*, pages 263–315, 1 2018.

[19] Ankur Choudhary. PharmaGuideline - Lubricant Concentration in Pharmaceutical Products. [Accessed October 2021].

[20] Yi Liu, Xiaolei Guo, Haifeng Lu, and Xin Gong. An investigation of the effect of particle size on the flow behavior of pulverized coal. *Procedia Engineering*, 102:698–713, 11 2015.

[21] Kerry Johanson. Effect of particle shape on unconfined yield strength. *Powder Technology*, 194(3):246–251, sep 2009.

[22] Arezou Rasti, Hamid Ranjkesh Adarmanabadi, Maria Pineda, and Jesse Reinikainen. Evaluating the effect of soil particle characterization on internal friction angle. *American Journal of Engineering and Applied Sciences*, 14:129–138, 02 2021.

[23] Sonia M. Razavi, James Scicolone, Ron Snee, Ashish Kumar, Johny Bertels, Philippe Cappuyns, Ivo Assche, Alberto Cuitiño, and Fernando Muzzio. Prediction of tablet weight variability in continuous manufacturing. *International Journal of Pharmaceutics*, 575:118727, 10 2019.

[24] CouncilOfEurope. *European Pharmacopoeia supplement 6.4*. European Directorate for the Quality of Medicine, 6th edition, 208. Tablets Monograph 0478.